Single-cell analysis of habituation in *Stentor coeruleus*

Deepa Rajan*[1], Tatyana Makushok*[1], Asa Kalish[1], Lilibeth Acuna[2], Alex Bonville[2], Kathya Correa Almanza[2], Brenda Garibay[2], Eric Tang[2], Megan Voss[2], Athena Lin[1], Kyle Barlow[3], Patrick Harrigan[3], Mark M. Slabodnick[1], Wallace F. Marshall[1]

[1]Department of Biochemistry and Biophysics, University of California San Francisco, San Francisco, CA, USA
[2]CCC Summer course, Center for Cellular Construction, San Francisco State University, San Francisco, CA, USA
[3]Integrative Program in Quantitative Biology, University of California San Francisco, San Francisco, CA, USA

* these authors made equal contributions

Lead Contact:
Wallace F. Marshall
wallace.marshall@ucsf.edu
@WallaceUCSF

SUMMARY:
Although learning is often viewed as a unique feature of organisms with complex nervous systems, single-celled organisms also demonstrate basic forms of learning. The giant ciliate *Stentor coeruleus* responds to mechanical stimuli by contracting into a compact shape, presumably as a defense mechanism. When a Stentor cell is repeatedly stimulated at a constant level of force, it will learn to ignore that stimulus, but will still respond to stronger stimuli. Prior studies of habituation in *Stentor* reported a graded response, suggesting that cells transition through a continuous range of response probabilities. By analyzing single cells using an automated apparatus to deliver calibrated stimuli, we find that habituation occurs via a single step-like switch in contraction probability within each cell, with the graded response in a population arising from the random distribution of switching times in individual cells. This step-like response allows *Stentor* behavior to be represented by a simple two-state model whose parameters can be estimated from experimental measurements. We find that transition rates depend on stimulus force and also on the time between stimuli. The ability to measure the behavior of the same cell to the same stimulus allowed us to quantify the functional heterogeneity among single cells. Together our results suggest that the behavior of Stentor is governed by a two-state stochastic machine whose transition rates are sensitive to the time series properties of the input stimuli.

INTRODUCTION

Habituation, in which organisms learns to ignore repetitive stimuli, is a form of learning found in most animals[1] . Habituation has been extensively studied in animals ranging from invertebrates to mammals[2-4] in which it is found that most instances show ten characteristics[5], among which are the response decreasing faster when the stimulations are more frequent and the spontaneous recovery of the response after the stimulation is stopped.

Intriguingly, habituation has also been observed in plants[6] and in individual free-living cells[7,8], including in bacteria[9] and in the polyploid plasmodium of the slime mold *Physarum polycephalum*[10]. Habituation has been particularly well studied in ciliate protists, whose large size and easily observable behaviors[11,12] , such as directed swimming and cell contraction, greatly facilitates the study of learning and behavior. Specific examples include *Spirostomum*[13], in which it has been shown that habituation does not require the presence of nucleus, and *Vorticella*[14], a ciliate that habituates to both mechanical and electrical stimuli. The ubiquity of habituation across such widely varying branches of biodiversity suggest it is somehow a fundamental property of living things.

What is the mechanism of learning in protists? In animals, habituation involves neuronal circuits in which the response of a neuron to the activity of other neurons is modified during learning[3]. In contrast, the molecular mechanism of habituation in single-celled organisms is less well understood. Habituation in single cells has been best studied in the ciliate *Stentor coeruleus*[15], which displays habituation to mechanical stimuli[16]. *Stentor* (**Figure 1A,B**) attach to surfaces and contract in response to stimulation (**Figure 1C**). Contraction takes a few milliseconds[17,18] while re-extension takes about a minute. If an identical stimulus is applied repeatedly, *Stentor* gradually stop responding, indicating they have habituated[11,16]. Weaker stimuli cause faster habituation than stronger stimuli[16]. Strong stimuli still elicit a contraction in habituated cells, and repeated strong stimuli prevent habituation, arguing against simple exhaustion as a mechanism. These features of habituation in *Stentor* match those seen in animal habituation[1,5].

Electrophysiological and drug treatment studies[19-21] have shown that mechanical stimulation triggers an initial membrane depolarization, which then triggers an action potential, leading to calcium influx that drives contraction mediated by fibers composed of calcium binding proteins. Repeated mechanical stimulation leads to a decrease in mechanoreceptor potential amplitude[20,21]. The molecular identity of the mechanosensory channel remains unknown, although its electrophysiological properties have been well studied by Wood. Mechanosensitivity is localized at the regions of the cell membrane overlaying stripes of blue pigment granules[22], indicating that the mechanoreceptor molecule is likely localized in these areas. Stimulation of one region of the cell surface leads to habituation of the cell as a whole, indicating that habituation is not simply local adaptation of individual stimulated mechanoreceptor molecules in response to their own individual activation[23].

Wood[21] has found that the action potential remains almost the same during habituation, whereas in contrast a much stronger effect is seen on the receptor potential, implying that haibutation works by modifying the properties of the ion channel associated with sensing the stimulus. Those studies indicated that the conductance of the receptor channel was reduced during habituation, and, importantly, that the effect was not due to decreased numbers of receptors, but to an alteration in their voltage dependence. Based on these results, Wood proposed a model for habituation in which a modification of the gating charge of the receptor associated channel, possibly due to phosphorylation. Such a model would naturally give a graded response, as various individual receptor channels became modified, leading to a gradual alteration in the voltage dependence, and a gradual change in mechanoreceptor potential amplitude. Such a gradual change in receptor potential would fit the gradual reduction in response probability seen in populations of cells[16].

Here, we quantified the response of individual cells during stimulation, and found that although the population response is graded, the response of individual cells is best accounted for by a step-like response, in which a cell can be in either of two states, with stochastic switching between the states.

RESULTS

Observation of single-cell response during habituation

Using an Arduino-controlled system to apply mechanical stimuli (**Figure 1D**; for details see Methods and **Figure S1)** we imaged *Stentor* cells subjected to a series of stimuli applied at uniform frequency, allowing us to visualize cells before and after stimulation (**Figure 1E,F**). Consistent with previous reports of habituation in *Stentor*[16] we observed that the fraction of cells contracting at each stimulation decreased over time (**Figure 1G**). Both the frequency of response and the habituation rate observed with our apparatus were comparable to those reported by Wood[16]. Also consistent with prior reports[16], we found that the fraction of cells contracting decreased more rapidly when weaker stimuli were applied (**Figure 1G,H**).

These results show that a population of cells habituates gradually to the stimulus. We next examined the responses of individual cells, by manually tracking cells through video images acquired during habituation. For each cell, we checked its contraction behavior at each stimulation, and recorded whether or not it contracted. **Figure 2A** gives representative examples of such recordings. The complete set of responses are given in **Figure S2A and B**. It is visually apparent that individual cells start out responding to a large fraction of the stimuli, and after maintaining this degree of response for some time, the responses become less frequent. This visual pattern suggested that cells might undergo a switch in response probability from a high response to a low response probability, thus giving a step-like response.

In order to test for a step-like response in an unbiased fashion, we implemented an algorithm to identify steps in the response pattern by testing partitions of each time series, to identify the time point at which the response probability before and after that point differ maximally. To perform this test (see Methods for details), each timepoint is considered as a possible step, and the fraction of cells contracting per stimulus before and after that time point are compared using Fishers exact test. The timepoint at which the test shows the maximal difference is taken as the location of the step. The inferred step points for two examples are indicated in **Figure 2A** by the line graphs. Out of 22 cells from three separate experiments using the same starting culture, 20 showed a statistically significant difference ($P<0.02$) in the response before and after the step point. As a control, we repeated the analysis on scrambled data in which the same set of responses for each cell were randomly permuted. As shown by the first two columns in **Figure 2B**, the minimum P values for scrambled data are much larger than for the original data, arguing that most cells show a statistically significant step transition in their response probability.

To determine whether additional steps take place other than the step defined above, we repeated the same procedure for the subset of time-points before and after the primary step. In each case, we asked if the resulting sub-partitions show a significant difference in contraction probability when split at any time point in their range. **Figure 2B** shows the distribution of p values for the two sub-partitions, which both show a similar range of values as for scrambled data. Neither prior to the original step-point, nor after the original step point, did any of the cells show a statistically significant difference in response within any sub-partition, suggesting that only a single step took place during the experiment.

However, a key question is whether the test employed here can discriminate a single step from a graded process. To ask this question, we simulated single-cell data using the population contraction probability in **Figure 1G**, and then analyzed the simulated datasets using the step detection algorithm. As shown in **Figure 2C**, the graded model produced a distribution of step p values that is skewed towards larger values, indicating cases in which no step was detected, but it does partially overlap the real data, indicating that in a number of cases the graded model produces apparent steps. Based on the distribution of scores for real versus simulated graded data, the single-step model provides a better fit to the real data than the graded model ($p=0.000034$, Mann-Whitney test for unpaired data), but because the graded model can in some

cases produce apparent steps, we cannot strictly rule out the graded model from this comparison alone.

As a further way to discriminate single-step from graded behavior, we asked how the dwell times in the responsive state are distributed. For each cell determined by **Figure 2B** to show a single step (n=18), we used an edge detector based on the step detection procedure, as described in Methods, to determine the time point at which the response first drops significantly below the initial response rate for each cell. The distribution of dwell times in the responsive state is plotted in **Figure 2D**. For a single-step process with a constant probability of switching per unit time, the dwell time histogram should show a geometric distribution. As shown by the orange bars in **Figure 2D**, the real data do in fact fit well to a geometric distribution ($\chi^2 = 0.86$, $p = 0.93$). We note that the geometric distribution plotted was not derived by fitting, but by using the inverse of the average dwell time taken directly from the experimental data. We also note that the mean dwell time estimated by this method is in good agreement with the half-time for decay of the response at the population level as plotted in **Figure 1G**. In contrast to the good fit between the single-step model (as judged by the geometric distribution), the step time distribution obtained from the simulated graded data in **Figure 2C,** indicated by the gray bars in **Figure 2D,** does not fit well with the experimentally observed step time distribution ($\chi^2 = 22.8$, $p=0.00014$). Taken together, our data show that the single-step model provides a better fit to the observed cell behavior than the graded model, particularly in terms of the step time distribution.

We repeated the same analysis for another 44 cells from the low force experiment of **Figure 1H**, with results given in **Figure S2B-E**. Unlike the case with the higher force regime, some cells did not show any obvious downward step in response, instead showing a uniformly low frequency of contracting throughout the course of the experiment. However, for the cells that did show a decrease in contraction probability during the course of the experiment, they only showed a single step, with no evidence for multiple stepping, and the dwell times in the responsive state again showed a distribution that was not significantly different from a geometric distribution, consistent with a uniform probability of switching states per unit time (**Figure S2E** orange bars, $\chi^2 = 3.2$, $p=0.53$). The step time distribution estimated from the population response to mimic a graded response (as was done above) did not fit the real data as well (**Figure S2E** grey bars, ($\chi^2 = 8.4$, $p=0.08$). In this case, the real data are potentially consistent with either the single-step (geometric distribution) or graded (distribution obtained from simulations using population data) models, however the quality of the fit is numerically better for the single-step model.

We conclude that while a population of *Stentor* cells shows gradual habituation, the response of individual cells may be better described by a single switch-like transition from a responsive to a non-responsive state, rather than a graded response. This observation immediately suggests a two-state model, which we consider next.

Two-state model for habituation in Stentor

Learning requires that the internal state of the system must change in response to past history. The simplest model for this process is a two-state model represented by the state-transition diagram of **Figure 3A**. In each of the two states, the cell has a fixed probability of contracting in response to the stimulus. State 1 represents a cell in a “responsive” state with a high probability of contracting, while State 2 represents a cell in a “non-responsive” state that is less likely to contract when stimulated. In between successive stimuli, the cell switches between the two states with some fixed transition probability, as suggested by the geometric distribution of stepping times (**Figure 2D)**. The probabilities of responding and of switching are both potentially functions of the stimulus strength. These types of state models have been used to

model decision making in humans and animals[24]. In our case, we assume that prior to the application of any stimulus, most of the cells are in State 1 (the responsive state), which would be the case if the forward transition rate p_{12} (from State 1 to State 2) is much lower than the reverse transition rate p_{21} (from State 2 back to State 1) in the absence of external stimulus. Habituation would take place if, in the presence of a stimulus, the transition probabilities shift such that the forward transition becomes more probable. This would cause some of the cells to switch into the non-responsive state, leading to the observed decrease in response. With continued stimulation, the population of cells would reach a steady-state distribution with the majority of cells in the non-responsive state but some cells in the responsive state.

At any given stimulus level, the model is characterized by four parameters: p_{12} describes the probability of switching from State 1 to State 2, p_{21} describes the probability of the reverse transition, and P_1 and P_2 are the probabilities of contracting while in state 1 or state 2, respectively. The schematic model of **Figure 3A** can be characterized by a differential equation that describes the probability of a cell being in State 1, as follows:

$$\frac{dP(State\ 1)}{dt} = p_{21}(1 - P(State\ 1)) - p_{12}P(State\ 1) \quad (1)$$

In this model, which is a continuous time version of the discrete transitions, the probability of contraction should show an exponential decay from an initially high response probability prior to stimulation to a steady-state response probability of

$$P_s = \frac{P_2 p_{12} + P_1 p_{21}}{p_{12} + p_{21}} \quad (2)$$

with a decay time of

$$\tau = \frac{1}{p_{12} + p_{21}} \quad (3)$$

Stochastic simulations of this model (**Figure 3B**) show that habituation is indeed observed, and that the change in response probability is approximated by an exponential. This simple two-state model is thus able to replicate the gradual decrease in response probability in a population of cells. Even though individual cells undergo a discrete switch from a high probability of response to a low probability of response, different cells undergo this switch at different times, and this results in a gradually reduced response in the population. We conclude from these simulations that the step-like responses of individual cells as described in **Figure 2**, involving just two states, are sufficient to explain the graded response in populations of cells as observed in **Figure 1**.

We note that we have formulated this model as a Discrete Time Markov Process, in which transitions occur at regular time intervals corresponding to moments when an input stimulus is received, such that the transitions rates p_{12} and p_{21} are unitless probabilities. In reality, there is no reason for a cell to be waiting for inputs at 1 minute intervals and so it is far more likely that the system is behaving as a Continuous Time Markov Process, in which there is a constant transition rate per unit time, with p_{12} and p_{21} reflecting the integral of the transition probability over the time interval between successive stimuli.

Using single-cell measurements to estimate parameters for the two-state model

The two-state model is characterized by four parameters. The habituation decay curve such as seen in experimental data of a population of cells can be fully characterized by three parameters - the initial response probability, the final response probability, and the decay time. The fact that the data can be described with just three parameters, but the model requires four

parameters, suggests that population level plots such as that in **Figure 1GH** may not contain enough information to reliably estimate parameter values in the model. Indeed, as shown in **Figure 3B**, different sets of parameter values can give apparently identical habituation results.

In order to provide additional information for fitting model parameters, we use our single-cell data to compute the run lengths for successive contractions or non-contractions of individual cells. Simulations of the two-state model show that run-time distributions (the number of contractions in a row or the number of non-responses in a row) can be different between sets of model parameters that have identical habituation responses (**Figure 3C,D**), showing that single-cell measurements may provide additional information for estimating model parameters compared to population level analysis.

We implemented a strategy for parameter estimation for the two-state model (detailed in Methods) in which we sweep parameters, carry out stochastic simulations, and compare the results with observed data based on a joint cost function involving the decay time, steady state contraction probability, and the first three moments of the steady state contraction and non-contraction run times. Simulations confirmed that this procedure is able to recover the parameter values used for the simulations.

We then combined the single cell data for one set of conditions (1 min between stimuli, 5.3 mm swing, which we refer to as "high force") and used the combined data (initial response, decay time, final response, and first three moments of single-cell contraction and non-contraction run time distributions) to estimate model parameters. **Figure 3E-G** shows the experimentally measured response for the high force experiment overlayed with the results of a simulation using the parameters obtained by our fitting procedure, confirming a close agreement**. Figure 3H-J** shows the model fit for data obtained using the low force stimulation. The results of the model fitting are summarized in **Figure 3K** which provides state transition diagrams that best predict the single-cell experimental results under the two force regimes. Two notable features are that the transition probability from the non-responsive state to the responsive state, p_{21}, is extremely small in both cases, and that the transition probability p_{12} from the responsive to the non-responsive state is higher for cells stimulated with lower force, consistent with the faster rate of habituation seen when weaker forces are applied[16]. The very small rate of transition p_{21} is consistent with the direct analysis of single-cell steps in **Figure 2** which suggests that once a step has occurred to the non-responsive state, it is highly unlikely for the cell to take a second step back to the responsive state.

To confirm the general features of this model, we repeated the analysis using 43 cells with a 2.5 minute interval between stimuli (**Figure S3).** When single cell data from these cells were used for fitting parameters of the two-state model, we found again that p_{21} was very small and that p_{12} was much larger for cells stimulated with a lower force (summarized in **Figure S3G**).

The transition rates and response probabilities of **Figure 3K** were obtained by parameter fitting using moments of the single cell run time distributions, an approach taken to ensure robustness in the face of relatively small numbers of measurements from individual cells. An alternative method is to directly estimate a hidden Markov model using the Baum-Welch algorithm[25] applied to the set of individual single-cell records. As shown in **Figure 3L**, when parameters were estimated using this methods, the results were qualitatively similar to the moment-based estimator, namely, it was found that the probability of the reverse transition, p_{21}, is extremely small for both high and low force, and the transition probability p_{12} is larger for lower forces.

Forgetting: state transition in the absence of stimulus

The fact that p_{21} is effectively zero is inconsistent with previous reports (16) that cells completely lose habituation in less than 1 hour after cessation of the stimuli. With our estimated values for p_{21} on the order of 0.001 min^{-1}, the habituated state should decay with a half-life of

approximately 5 hours, far slower than what Wood has reported. This raised the possibility that the rate of transitioning from the non-responsive state to the responsive state might itself be a function of the applied stimulus. To address this possibility, we carried out the experiment shown in **Figure 4A**, in which we applied a high-force stimulus once per minute for 30 minutes, then waited 15 minutes without applying any force, after which the stimulus was resumed for 5 more minutes. As shown **in Figure 4B**, we found that within 15 minutes, 90% of habituated cells became fully responsive again, from which we can calculate a transition rate of 0.15 min^{-1}. This is two orders of magnitude larger than the value of p_{21} estimated above in our two-state model. We note that the two values of p_{21} both describe the transition probability in the absence of a stimulus - in the normal experiment the transition occurs during the 1 min intervals between stimuli, and in the experiment of **Figure 4B**, it occurs during the 15 min interval after the stimulus train. Our results indicate that the transition rate is not constant per unit time, but increases as a function of elapsed time after the last stimulus, such that if stimuli continue to occur within some minimal timescale, the habituated state is maintained indefinitely, but when the stimulus is missing for a longer period, the habituated state is lost. This type of behavior is often employed in an engineering context in the form of a "watchdog timer" which continuously resets itself as long as some input continues to be received, but then triggers a different response when no input occurs during the desired time interval. We speculate that the maintenance of habituation in *Stentor* may involve a molecular analog of such a watchdog timer mechanism. A biological example is the exonuclease activity of DNA polymerase, which is normally inactive and only triggered when the time between successive nucleotide incorporation events becomes long[26]. We also note that the fact that transitions occur even when stimuli are not being applied confirms that the reverse transition is taking place as a continuous time, rather than discrete time, process.

State transitions in a higher force regime

Wood[16] has reported that with sufficiently strong stimuli, habituation takes place very slowly if at all. We analyzed contraction of single cells in a higher force regime generated by a stepper motor (**Figure 4C-F,** see Methods) under which habituation was approximately 3-6 times slower than in the lower force examples in **Figure 1**. Applying the step detection algorithm, out of 20 cells examined, all 20 showed a single statistically defined step according to our procedure (**Figure 4E**). One cell showed potential support for a second step after the primary step, but with a much lower degree of statistical support than the primary steps for any of the 20 cells. Analysis of step time distributions (**Figure 4F**) showed a dramatic difference at high forces compared to the previous data in **Figure 2**. Instead of a geometric step time distribution in which most of the steps took place within the first 5 stimuli, we observed a step time distribution with a clear peak in stimuli 5-10. This peaked distribution was well fit with an Erlang distribution having shape factor 5 (χ^2 = 0.86 p=0.83). In contrast, a simulated step time distribution representing a graded response by simulating contractions using population data did not fit the actual step time distribution (χ^2 = 9.8 p=0.04). These results indicate that even at a very high force, habituation takes place through a single state transition, but unlike at lower forces, at high force the probability of transition p_{12} is no longer constant per unit time. Erlang distributions typically arise in processes where an observable transition requires multiple independent, unobserved transitions, with the shape factor indicating the number of unobserved independent transitions.

State transitions at higher stimulus frequency

The "forgetting" experiments of **Figure 4A-B** indicate that the reverse transition rate p_{21} is a function of stimulus frequency. To ask whether the forward transition rate p_{12} might also depend on frequency, we applied stimuli at a period of 1.2 seconds (**Figure 4G**) using the same force as **Figure 4C**. The result was dramatically faster habituation. Within 2.5 minutes, the cells had

switched to the nonresponsive state, representing at least an order of magnitude faster habituation compared to that seen when stimuli were applied at a period of 1 min (**Figure 4C**). As noted above, two state model of **Figure 3A** did not specify whether transitions took place only at discrete times when stimuli arrive, or continuously over time. In the former case, we would expect that habituation with higher frequency stimuli might take place with a similar number of stimuli, while in the second case it would require a higher number of stimuli for a transition to occur, since less time elapses between them. As shown in **Figure 4H**, when we plot contraction versus stimulus number for the 1 min and 1.2 second stimuli, it is apparent that a higher number of stimuli are required to achieve the state transition with 1.2 seconds between stimuli, arguing against the idea that state transitions occur only at the arrival of stimuli. However, as shown in **Figure 4I**, the rate of habituation as a function of time is clearly higher when the stimuli arrive at higher frequency.

We conclude that, as with reverse transitions (forgetting) that can take place in between stimuli and for which the magnitude of the rate p_{21} is a function of stimulus frequency, the same is true for the forward transition (habituation). But in contrast to p_{21}, which decreases with stimulus frequency, p_{12} increases with stimulus frequency. It is interesting to consider whether cells might have a single timer or other mechanism that tracks stimulus frequency and modulates both p_{12} and p_{21} accordingly.

Stentor does not anticipate stimuli

One potentially confounding effect not included in the two state model could occur if cells learn to anticipate the next stimulus, as has been demonstrated for *Physarum*[27]. Under our imaging conditions, spontaneous contractions are extremely rare. But given the period nature of our stimulus, cells might learn to contract periodically, something that is not included in the two state model. In order to test for such anticipation directly, we performed the experiment of **Figure S4A** in which cells were subjected to a train of high-force stimuli with a period of 1 minute, after which the stimulus was stopped and the response monitored at the next 1 minute interval. In this experiment, none of the cells contracted when the stimulus was removed (**Figure S4B**), arguing that anticipation is unlikely to be a major factor in the contraction response.

Heterogeneity in cell behavior at steady state

The two-state model as formulated assumes that all cells have the same contraction probability as other cells in the same state. Because cells appear to remain in the non-responsive state after switching, we can test this assumption for the non-responsive state. As shown in **Figure S4C,D**, the distribution of contraction counts in the non-responsive state (which we assume for cells at timepoints 20 and above) clearly does not match a Poisson distribution, potentially indicating heterogeneity among cells. Selecting timepoints for steady state as described in Methods, the average number of contractions for low and high force were 1.3 and 6.1, with variances of 2.1 and 25 respectively. The fact that the variance to mean ratios are substantially greater than 1 confirms that the contractions do not obey a simple Poisson distribution.

These data suggest that cells do not all have the same probability of contraction. If we assume that each cell has a constant probability of contraction, but that these probabilities vary randomly from cell to cell, the result is a Poisson mixture model, in which the distribution of contractions observed in a population of cells consists of a weighted sum of individual Poisson distributions having different Poisson parameters corresponding to different probabilities of contraction. As outlined in Methods, the mean and variance of the distribution of Poisson parameters in such a mixture model can be estimated from the mean and variance of the observed numbers of contractions in a collection of individuals. Using this approach together with the mean and variances reported above, we calculate the coefficient of variation for the

contraction probabilities (see Methods) to be approximately 0.7 for both force regimes, suggesting less than two-fold variation across different cells.

DISCUSSION

Summary of results

By collecting data on the behavior of single Stentor cells during stimulation by a computer-controlled apparatus, we found that the graded habituation response previously reported for populations of cells reflects step-like behavior of individual cells. These data lead to a simple two-state model, in which individual cells step from a responsive to a non-responsive state with transition probabilities that depend on the force and frequency of the stimuli. The transitions in this model occur continuously in time and not just when stimuli are applied. For very large stimulus forces, the step time distribution for the forward transition suggests multiple underlying steps. The ability to observe individual cells responding to repeated stimulation allowed us to calculate the heterogeneity of the response, showing a less than two fold difference in response probabilities from cell to cell.

Force-dependence of state transition rates

It has previously been shown[16], and we have confirmed, that habituation is slower in response to larger stimuli. In the context of our two-state model, either the rate of transitioning from responsive to nonresponsive states (p_{12}) must be smaller with large forces, or the rate of transitioning back to a responsive state from the nonresponsive state (p_{21}) must be larger. Based on the parameter values estimated in **Figure 3K,L** and **Figure S3G**, we find that when force is reduced, p_{12} and p_{21} both increase by a factor of about two. Only the increase in p_{12} can contribute to the increased speed of habituation at low force, since an increase in p_{21} would lead to faster forgetting rather than faster habituation, and in any case p_{21} remains very small even in the low force experiments. We conclude that the effect of force on habituation rate first noted by Wood is due to an effect on the transition rate p_{12}.

Comparison to other studies of Stentor behavior and learning

Our work confirms the previously reported dynamics of habituation in populations of *Stentor* cells[16,19] but differs from these previous reports by analyzing single-cell response data, which allowed us to show that the apparent graded response previously reported actually results from step-like behavior. Wood[19] showed that during habituation, the mechanoreceptor depolarization in a population of cells decreased while the action potential remained the same. Since the receptor induced depolarization is presumably what determines the triggering of the action potential, the decrease in this potential observed by Wood is consistent with the switch to a lower probability of response in our model.

Stentor roeselli, a close relative of *Stentor coeruleus*, responds to stimuli using three possible escape mechanisms (bending, ciliary reversal, and contraction), which it employs sequentially[11,12,28]. A simple two-state model like we propose could produce a different set of responses in the two states, but would not permit the cell to show differential habituation rates for distinct responses, and would not produce the sequential use of different responses that has been seen. Future studies with *Stentor coeruleus* may expand our two-state model to incorporate other escape mechanisms beyond contraction. Considering just the contraction response of *S. roeselli*, Jennings only gave examples of the responses of several individual cells, but in these few examples a single step in contraction probability is visibly apparent[11].

Possible molecular basis of the two-state model

There are many possible molecular implementations of a two state model such as that described here[29]. In the specific case of *Stentor* habituation, almost any component of the stimulus-response pathway, from sensor to effector, could be the key molecule that undergoes a state switch to take the cell from a responsive to less responsive state. We know that mechanosensitive ion channels are involved in the variable response[21], and that EF-hand

calcium-binding protein fibers drive the mechanical contraction[30,31]. Both mechanosensitive channels and EF-hand proteins are known to be regulated by phosphorylation[32-34], and either could provide the basis of reduced response probability if modified during habituation.

Wood[21] has shown clearly that the voltage dependence of the mechanoreceptor associated channel changes during habituation, making this by far the most likely candidate for the substrate of learning in *Stentor*. In order to achieve a step-like switch in response probability, it would somehow be necessary for all of these channels to be modified in a coordinated way. Such coordination, together with the apparent involvement of timers in setting the transition rates in between successive stimuli, suggest that complex molecular computation may be taking place upstream of the receptor modification, as opposed to a simple gradual accumulation of phosphorylations.

ACKNOWLEDGMENTS:
This work was an outgrowth of experiments started in the UCSF Cellular Cognition Minicourse 2012. We acknowledge stimulating discussions with the students in that course as well as in subsequent years of the same course and in the Physiology Course at the Marine Biological Laboratory in Woods Hole. We also thank current and former members of the Marshall lab, as well as Rob Phillips, Tao Long, Kurt Thorn, Nicholas Ingolia, Adam Frost, and Steve Beckwith, for discussions about this project. This work was supported by NSF grant MCB- 2012647 and NIH grant R35 GM130327. Work from students in the CCC summer course was supported by NSF grant DBI-1548297. Initial work on this project was supported by a new frontiers award from the UCSF Program in Breakthrough Biomedical Research.

AUTHOR CONTRIBUTIONS:
The apparatus used in this work was designed and built by W.F.M. Experiments were performed by D.R., T.M., L.A., A.B., K.C.A., B. G., E. T., M.V., K.B., P.H., M.M.S., and W.F.M. Software to run the apparatus and analyze data was developed by K.B., P.H., and W.F.M. Data was analyzed by T.M., D.R. A.K., and W.F.M.. Figures were prepared by T.M., A.L., W.F.M., and D.R., T.M., W.F.M. wrote the paper.

DECLARATION OF INTERESTS
The authors declare no competing interests.

INCLUSION AND DIVERSITY
We support inclusive, diverse, and equitable conduct of research

Figure Legends

Figure 1. Confirming habituation in *Stentor coeruleus* using an Arduino-controlled device. (**A**) Image of *Stentor coeruleus* cell. Scale bar 200 μm. (**B**) Diagram showing key anatomical features. Immediately beneath the ciliary rows are myonemes, contractile filaments that can drive a rapid change in cell shape. (**C**) When a *Stentor* cell is mechanically stimulated, for example by contact with a predator, the cell contracts into a ball. If a cell has been repeatedly stimulated and thus habituated, it will ignore the stimulus and remain in its elongated shape. (**D**) Diagram of apparatus for testing *Stentor* habituation. Cells are placed in a petri dish attached to a metal strip. An electromagnet is positioned to deflect the metal strip downward when energized, thus providing a mechanical stimulus to the cells in the dish. Two mechanical stops determine the range of motion and thus the level of force applied to the cells. (**E,F**) Image of *Stentor* cells before (**E**) and after (**F**) applying a mechanical stimulus using the device. The cells can be seen to have contracted into a more compact shape. Scale bars 1 mm. (**G**) Fraction of cells contracting after each of 30 stimuli applied at 1 min intervals. The stops were adjusted to produce a large deflection (5.3 mm) of the metal strip, thereby creating a large force stimulus. Habituation is indicated by the gradual reduction in the probability of cells contracting with successive stimuli. Data shown are the aggregate results of three independent experiments, with a total of 31 cells. Error bars indicate standard error calculated from the Bernoulli distribution. (**H**) Fraction of cells contracted per stimulus in a separate set of experiments in which the stops were adjusted to produce a smaller deflection (4.0 mm) and thus a lower force stimulus. Data shown are the aggregate results of four separate experiments with a total of 44 cells. Error bars indicate standard error. Additional information about the apparatus is provided in **Figure S1**.

Figure 2. ***Stentor* habituation in single cells occurs via a single step in response probability.** (**A**) Examples of single cell data. Grid bars indicate response of individual cells to successive stimuli at the high force regime corresponding to **Figure 1G**. Line graphs below the grid bars indicate the steps inferred using Fishers exact test as described in the main text. (**B**) P values for Fisher's exact test for the optimal step, and for the optimal second steps inferred for the two sub-partitions created by the first step. For each cell, a control was generated by randomly permuting the data and applying the same test. Note that P values are plotted on a log scale. N=22. The much smaller P values for the first step compared to the scrambled data indicate the step is not a statistical artifact of the analysis procedure. The lower P values for the first step compared to the putative steps identified before or after the main step, indicate that the cells are predominantly taking just a single step. (**C**) Results of applying step analysis to simulated graded response data generated according to the experimental probabilities of contraction at each time point from the population data of **Figure 1G**. Larger P values indicate weaker evidence for a step. (**D**) Step time distribution for experimental data (blue) compared to a geometric distribution based solely on the mean step time (orange) and to the step time distribution obtained from the mock data of panel C simulating a graded response (grey). Note that the geometric distribution was not fit to the data but calculated from the average step time. The first bin, listed as a dwell time of zero, denotes cells for which no step was detected. Step analysis of another 44 cells, subject to the low force stimulus, as per **Figure 1H**, are given in **Figure S2**.

Figure 3. **Two-state model for *Stentor* habituation can account for observed habituation dynamics.** (**A**) In the two-state model, a cell can be in either of two states, responsive or non-responsive, which we label as states 1 and 2, respectively. Between successive stimuli, the cell can switch from one state to the other with specified transition probabilities p_{12} and p_{21}, which denote the probability of switching from state 1 to state 2, or from state 2 back to state 1,

respectively. Within each state, the cell has a given probability of contracting when stimulated. We denote the probability of contracting when stimulated while in states 1 or 2 as P_1 and P_2 respectively. (**B**) Stochastic simulation of the two-state model. The transition diagrams give two different parameter sets which produce the same population level habituation response as shown by the graph. The color of the dots in the graph corresponds to the color of the text in the two state diagrams to the left. (**C**) Steady-state run length distribution for successive contraction events, for simulations using the two parameter sets from panel B. The distribution is calculated once the population level data has reached its final plateau in order to focus on the steady state condition. Although these two sets of parameters gave identical results for the habituation plot in panel B, they give different run length distributions and can therefore be distinguished using single cell data. (**D**) Run length distribution for successive non-contractions. Again, the two parameter sets that gave identical population responses in Panel B can be distinguished based on single cell data in the form of non-contraction run length distributions. (**E,F,G**) Fitting experimental data using high force stimulus to the two-state model. The model was simultaneously fit to the population response data (**E**), the steady-state run length distribution of successive contractions (**F**), and the steady-state run length distribution of successive non-contractions (**G**). Experimental data in blue reflects 153 contraction runs and 153 non-contraction runs. Simulation results for the best-fit two state model are shown in the red line in panel E and the orange bars in panels F and G. (**H,I,J**) Fitting experimental data using low force stimulus to the two-state model. Experimental data in blue reflects 141 contraction runs and 141 non-contraction runs. (**K**) Two-state models inferred for high and low forces. (**L**) Two-state model inferred for high and low force using the Baum-Welch HMM estimation algorithm as described in Methods. A completely separate set of experiments using two different force levels with a 2.5 min interval between stimuli is given in **Figure S3**.

Figure 4. Dynamics of state transitions. (**A**) Testing the timescale over which *Stentor* forgets its habituated state. Diagram depicts experiment in which successive stimuli are applied until the cells become habituated, after which the stimulus is paused for 15 minutes. The stimulus is then resumed and the response recorded. (**B**) Fraction of cells contracting at the start of the experiment, at the end of the habituation period, and at the first stimulus after the pause. (N=32,29, and 24 respectively). Error bars show standard error calculated from a Bernoulli distribution. (**C**) Response of cells to a higher force stimulus generated with a stepper-motor based device. N=20. (**D**) Individual cell responses for the cells of panel C. (**E**) Step detection results for the cells of panel C. (**F**) Step time distribution for the higher force data of panel C (blue) compared to an Erlang distribution with k=5 (orange) and a predicted graded response obtained by applying the step detector to data simulated from the population data of panel C. (**G**) Response of cells to stimuli applied at a period of 1.2 seconds. (**H**) Comparing 1.2 seconds versus 1 min responses (panels C versus G) as a function of stimulus number. (blue) 1 min stimulus period, (red) 1.2 seconds stimulus period. (**I**) Comparing 1.2 seconds versus 1 min responses (panels C versus G) as a function of time. Additional information regarding the dynamics of memory formation, specifically concerning the question of anticipation, is provided in **Figure S4**.

STAR METHODS

RESOURCE AVAILABILITY

Lead contact: Requests for further information or resources should be directed to the lead contact, Wallace Marshall, wallace.marshall@ucsf.edu

Materials availability: This study did not generate any new unique reagents.

Data and code availability:

- All data reported in this paper will be shared by the lead contact upon request.
- All original code has been deposited on Github and is publically available. https://github.com/WallaceMarshallUCSF/StentorHabituation. The DOI (10.5281/zenodo.7262341is listed in the Key Resources Table.
- Any additional information required to reanalyze the data reported in this paper is available from the lead contact upon request.

EXPERIMENTAL MODEL AND SUBJECT DETAIL

Stentor coeruleus cells, originally obtained from Carolina Biological (Burlington, NC) were grown in filtered spring water and fed using a previously described feeding protocol[35] with the exception that cells were fed *Chilomonas*, also obtained from Carolina Biological, as opposed to *Chlamydomonas*. The number of mating types in *Stentor* has not yet been determined, nor do any methods exist to determine mating type, so we are unable to report this information for our cells.

METHOD DETAILS

Apparatus to analyze Stentor habituation

The habituation device (**Figure S1A**) consists of a steel strip (12 inch metal ruler) clamped to a post (Thorlabs P14) and free at the other end. A 35 mm petri dish (Benz Microscope Optics Center, L331) containing *Stentor* cells is anchored to the top of the strip with double-stick tape. Below the free end, an electromagnet (E-28-150, Magnetic Sensor Systems, Van Nuys, CA) is positioned 1 cm from the strip (**Figure S1B,C**). When the magnet is energized, the end of the steel strip is drawn downwards. An adjustable mechanical stop determines the extent of the motion, and thereby controls the strength of the stimulus applied. The position of the stop is adjusted by a micrometer (Thorlabs PT1). Activation of the magnet is controlled using an Arduino coupled with a custom control circuit (**Figure S1D,E**) consisting of a MOSFET (IRF510, Radio Shack) and flywheel diode to control the electromagnet, an LED to indicate when the system is running, set to flash five seconds before each stimulus, and two switches to manually trigger the magnet for setup and demonstration purposes. A USB microscope (Celestron 44308) mounted on a ring-stand is used to image the cells during the experiment. **Figure S1F** shows a calibration curve relating the distance moved by the tip of the metal strip to the fraction of cells that contract on the first stimulus. Experiments done in the "high force" regime were performed with the micrometer set to produce a swing of 5.3 mm. For the "low force" regime, the swing was adjusted to 4.0 mm. These swings were chosen so as to be low enough in magnitude to permit habituation, while being large enough in magnitude to produce a sufficient number of contractions at least for the first several time-points. The reason that the two setting differ by 1.3 mm is that the micrometer is calibrated in tenths of an inch, thus these two setting correspond to adjacent major lines on the micrometer handle. For the experiments to detect anticipation in **Figure 4AB**, the swing was 6.6 mm, chosen large enough to ensure that the majority of cells would contract when stimulated and that habituation would not take place. The Arduino program that runs the habituation device is available on github (https://github.com/WallaceMarshallUCSF/StentorHabituation). For the experiments of **Figure**

4C and 4G, a modified version of the device was used in which the force on the metal ruler was generated by a stepper motor rather than an electromagnet. Due to the rapid motion of the motor compared to the slower response of the metal strip to the magnet, this devices allowed stimuli to be applied at higher forces and frequencies than the magnet based device.

Setup of apparatus for habituation experiments

For each experiment, 1 mL of media from the *Stentor* culture was added to a 35 mm petri dish with a circular pieces of glass fiber filter (Omicron Scientific 133047) cut to size and placed on the bottom, which encourages attachment of the cells. 10-20 cells were then added to the media in the dish using a pipette in a volume of approximately 1mL making the total volume in the dish 2 mL. The apparatus was set up and then allowed to sit for 8 hours with the cells in place, with the dish covered, without any mechanical stimulation, to allow them to recover from being transferred to the dish and to adapt to the new environment. Experiments were performed under uniform illumination, making sure room lights stay on during the pre-adaptation phase. This is necessary because *Stentor* demonstrates a strong photophobic response as well as adaptation to light[36].

For experiments involving the stepper motor apparatus, the same procedure was followed with a few exceptions: The cells were fed *Chlamydomonas*[35] rather than *Chilomonas*, and each experiment involved 100 cells in a total volume of 4 mL filtered spring water within the 35 mm petri dish. No glass fiber filter was used because the petri dish was instead manually coated with 0.01% poly-ornithine solution (Millipore Sigma, P4957) overnight to facilitate anchoring of cells to the bottom of the plate. For the experiment in **Figure 4C**, the cells were allowed to sit for 2 hours without any mechanical stimulation prior to the start of the experiment. For the experiment in **Figure 4G**, the cells were allowed to sit overnight without perturbations. The cells cannot be exposed to any mechanical stimuli for a minimum of 2 h before the start of a habituation experiment because the *Stentor* forgetting timescale after experiencing mechanical stimulation is 2-6 hours[16].

Measurement of cell contractions

In order to score cell contractions, images are acquired within 5 seconds before the start of each image, and then 5 seconds after, allowing the response of each cell to be determined. Cells are manually tracked between successive images. Only cells that were continuously attached to the substrate during the whole experiment were scored. Any cells that detached and swam away were excluded from analysis, as were any cells that swam into view and then became attached after the experiment had begun. These cells were excluded in order to avoid potential complications if the response of cells swimming, or their perception of the mechanical stimulus, is different from cells while attached. We also applied these criteria to the cells in the high-frequency learning experiments in **Figure 4G**, although a few cells detached over the course of the experiment because the high density of cells precluded unambiguous detection of each detached cell – however, the vast majority remained attached for the entirety of the experiment. We only observed two cells that were undergoing cell division during any of the experiments, and these were also excluded. In some cases, a cell could be seen to stay attached through the course of the experiment but it was not possible to unambiguously determine its contraction state at some time points due to interference from debris on the dish. In those cases, the contraction of the cell was included in population-level plots for any time point at which the cell could be observed. Such cells were, however, excluded from the single cell run-time analysis because the missing time-points would create ambiguity in the run time distributions.

Because the apparatus involves bending a metal strip with the petri dish attached, the dish is tilted during the experiment such that regions of the dish nearer to the end of the strip will undergo a somewhat larger vertical deflection. To test whether this difference in vertical

deflection leads to a difference in cell stimulus, we divided the field of view into two halves and compared the probability of cells contracting in the half of the field of view closer to the clamped end of the strip versus in the half of the field of view closer to the moving end of the strip. We then quantified the fraction of cells contracting in the two half fields of view. As shown in **Figure S1G**, the difference in contraction probability was not significantly different. Probabilities were compared using a 2x2 contingency table test with Fisher's exact test, with p values given in the figure legend.

QUANTIFICATION AND STATISTICAL ANALYSIS

Automated detection of steps in response probability

Statistical analysis of step-like transitions in response probability was performed using a custom R program. For each data record from a single cell, each time point was examined sequentially. At each time point, Fisher's exact test was used to compare the proportion of cells contracting per stimulus before (and including) that time point versus the proportion of cells contracting after that time point. The time point at which the p value from Fisher's test was minimum was defined as the time of stepping. To test whether only a single step was present, each of the two sub-partitions of the data record, before and after the stepping time point, were re-examined using the same procedure and the minimum p value for sub-partitioning each of the initial partitions was recorded. The $\log_{10}$ of the p values are plotted in the beeswarm plots, noting that the Y axis is scaled differently for different experiments as indicated.

To obtain distributions of step times, an edge detection method was implemented using the same procedure was followed except that the first timepoint at which the p value dropped below 0.01 was taken as the step time. This procedure was used because as the time point increases, larger numbers of timepoints are included before the point of interest, such that the p value continues to decrease. In a comparison of the edge finding method versus the Fishers test method applied to simulated single-step data based on the parameters estimated in **Figure 3K**, the correlation coefficients between the step times estimated by the two methods compared to the actual step time in each simulation run were 0.73 and 0.52 for the edge detector and Fisher methods, respectively, suggesting that the edge detector gives a better estimate. This analysis was applied to all cells in each dataset regardless of whether a step was detected using the previous method. Cells for which no step was detected, based on the failure of the p value to drop below 0.01, were assigned a dwell time of zero. These data were included to allow for comparison between real data and different models, as described.

Numbers are given in figure legends and test statistics are reported in the main text Results section.

Quantifying heterogeneity in single-cell responses

To model heterogeneity, we assume that each cell has some probability of contracting, and that this contraction probability varies randomly from cell to cell. For any given cell, we assume that responses to successive stimuli are independent of each other, such that the number of contractions observed during the course of an experiment in a single cell, X, is assumed to follow a Poisson distribution. This distribution is characterized by a parameter λ that is equal to the average number of contractions expected if the experiment was repeated many times. Because the underlying contraction probabilities are different from cell to cell, the Poisson parameter λ is itself a random variable with some unknow distribution. The resulting model is thus a Poisson Mixture model. The variability in the values of λ for different cells is a way to quantify the degree of heterogeneity.

For Poisson mixtures[37] the variance and mean of the Poisson parameter λ are related to the variance and mean of the experimental outcomes according to the following two equations

$$E[X] = E[\lambda]$$

$$\sigma^2(X) = E[\lambda] + \sigma^2(\lambda)$$

From which we derive

$$\sigma^2(\lambda) = \sigma^2(X) - E[X]$$

Finally, to characterize heterogeneity, we calculate the coefficient of variation for the Poisson parameter λ as follows:

$$c_v(\gamma) = \frac{\sqrt{\sigma^2(X) - E[X]}}{E[X]}$$

Since the number of contractions is proportional to the contraction probability times the number of trials, the coefficient of variation in contraction probabilities is the same as the coefficient of variation in Poisson parameters, and this is the value reported in the Results. From our single cell measurements, we count for each cell the number of contractions taking place after timepoint 20, by which time we assume steady state has been reached. The counts are then used to compute E[X] and var(X). Numbers are reported in the main text Results section.

Stochastic simulations and parameter estimation from moments of run-lengths

Simulations of the two-state model were carried out in MATLAB using a custom program that tracks the state of each cell and switches from one state to another with the given probability at each time step of the simulation. For parameter estimation, simulations were run by sweeping parameter values at equal intervals. p_{21}, p_{12}, and P_2 were swept, while P_1 was set equal to the observed probability of contracting at the first stimulus. For each parameter combination, 500 cells were simulated for 500 time intervals and results compared to eight derived quantities for each experiment: decay time, fraction of cells contracting at steady state, the first three moments of the distribution of successive runs, and the first three moments of the distribution of successive non-runs. The use of moments to describe the run lengths was based on the idea that observed runs will represent a mixture of cells in two different states (responsive or non-responsive) and thus the overall distribution of run lengths should be approximately a mixture of exponentials. It has been shown that the first three moments of a two-exponential distribution can be sufficient to estimate the shape of the distribution[38].

Hidden Markov model parameter estimation

As an alternative to the moment-based estimation using simulations, we also estimated two-state model parameters using the Baum-Welch algorithm to estimate hidden Markov models from multiple input sequences[25]. For each force condition, individual cell records were truncated so that each cell dataset had the same number of time points, and the outcomes contract and non-contract were denoted by the symbols 2 and 1. These data were then used as input for the hmmtrain() function in Matlab, using [0.5,0.5;0.5,0.5] as the initial estimate for the transition probability matrix (i.e. making no initial assumption about transition rates) and using $[0.2, 0.8;\ \ 0.9, 0.1]$ as the initial estimate for the emission matrix to reflect approximate frequencies of contraction and non-contraction at the start and end of the experiment. The final result was completely insensitive to the specific values used in the initial guess emission matrix except that the emission probability for symbol 2 needed to be initialized to a large probability in

state 1 than in state 2, in order to maintain a consistent definition of state 1 referring to the higher probability of contracting state.

References

1. Thompson, R.F., and Spencer, W.A. (1966). Habituation: a model phenomenon for the study of neuronal substrates of behavior. Psych. Rev. *73*, 16-43.

2. Harris, J. D. (1943). Habituatory Response Decrement in the Intact Organism. Psychological Bulletin. *40*, 385-422.

3. Castellucci, V.F., Pinsker, H., Kupferman, I., and Kandel, E.R. (1970). Neuronal mechanisms of habituation and dishabituation of the gill-withdrawal reflex in Aplysia. Science *167*, 1745-1748.

4. Thompson, R. F. (2009). Habituation: A history. Neurobiology of Learning and Memory. *92*, 127-134.

5. Rankin, C. H. et al. (2009). Habituation revisited: an updated and revised description of the behavioral characteristics of habituation. Neurobiol Learn Mem. *92*, 135-138.

6. Gagliano, M., Renton, M., Depczynski, M. and Mancuso, S. (2014). Experience teaches plants to learn faster and forget slower in environments where it matters. Oecologia. *175*, 63-72.

7. Baluska, F., and Levin, M. (2016). On Having No Head: Cognition throughout Biological Systems. Front Psychol. *7*, 902.

8. Tang, S.K.Y., and Marshall, W.F. (2018). Cell Learning. Curr. Biol. *28*, R1180-1184.

9. Lyon, P. (2015). The cognitive cell: bacterial behavior reconsidered. Front Microbiol. *6*, 264.

10. Boisseau, R.P., Vogel, D., and Dussutour, A. (2016). Habituation in non-neural organisms: evidence from slime moulds. Proc. R. Soc. Lond. B *283*, 20160446.

11. Jennings, H.S. (1902). Studies on reactions to stimuli in unicellular organisms. IX. On the behavior of fixed infusoria (Stentor and Vorticella) with special reference to the modifiability of protozoan reactions. Am. J. Physiol. *8*, 23-60.

12. Dexter, J. P., Prabakaran, S., and Gunawardena, J. (2019). A Complex Hierarchy of Avoidance Behaviors in a Single-Cell Eukaryote. Curr. Biol. *29*, 4323-4329.e2

13. Applewhite, P.B., Lapan, E.A., and Gardner, F.T. (1969). Protozoan habituation learning after loss of macronuclei and cytoplasm. Nature *222*, 491-492.

14. Patterson, D. J. (1973). Habituation in a protozoan Vorticella convallaria. Behaviour. *45*, 304-311.

15. Tartar V. (1961). The Biology of Stentor. Pergammon Press.

16. Wood DC. (1970a). Parametric studies of the response decrement produced by mechanical stimuli in the protozoan, Stentor coeruleus. J Neurobiol. *1*, 345-360.

17. Jones, A. R., Jahn, T. L., and Fonseca, J. R. (1970). Contraction of protoplasm. III. Cinematographic analysis of the contraction of some heterotrichs. J. Cell Physiol. *75*, 1-7.

18. Newman, E. (1972). Contraction in Stentor coeruleus: a cinematic analysis. Science *177*, 447-449.

19. Wood DC. (1970b). Electrophysiological correlates of the response decrement produced by mechanical stimuli in the protozoan, Stentor coeruleus. J. Neurobiol. *2*, 1-11.

20. Wood DC. (1988a). Habituation in Stentor: a response-dependent process. J Neurosci. *8*, 2248-2253.

21. Wood DC. (1988b). Habituation in Stentor: produced by mechanoreceptor channel modification. J Neurosci. *8*, 2254-2258.

22. Wood, D. C. (1989). Localization of mechanoreceptors in the protozoan, Stentor coeruleus. J Comp Physiol A. *165*, 229-235.

23. Wood, D.C. (1972). Generalization of habituation bewteen different receptor surfaces of Stentor. Physiol. Behavior *9*, 161-165.

24. Busemeyer, J.R., and Diederich, A. (2009). Cognitive modeling. Sage Publications.

25. Rabiner, L.R. (1989). A tutorial on hidden Markov models and selected applications in speech recognition. Proc. IEEE *77*, 257-286.

26. Kunkel, T.A., and Bebenek, K. (2000). DNA replication fidelity. Annu Rev Biochem. *69*, 497-529.

27. Saigusa, T., Tero, A., Nakagaki, T., and Kuramoto, Y. (2008). Amoebae anticipate periodic events. Phys. Rev. Lett. *100*, 018101.

28. Trinh, M.K., Wayland, M.T., and Prabakaran, S. (2019). Behavioral analysis of single-cell aneural ciliate, Stentor roeseli, using machine learning approaches. J. R. Soc. Interface *16*, 20190410.

29. Phillips R. (2020). The molecular switch: Signaling and Allostery. Princeton University Press.

30. Huang B, Pitelka DR. (1973). The contractile process in the ciliate, Stentor coeruleus. I. The role of microtubules and filaments. J. Cell Biol. *57*, 704-28.

31. Maloney, M., McDaniel, W., Locknar, S., and Torlina, H. (2005). Identification and localization of a protein immunologically related to caltractin (centrin) in the myonemes and membranelles of the heterotrich ciliate Stentor coeruleus. Journal of Eukaryotic Microbiology, *52*, 328-338.

32. Wegierski, T., Lewandowski, U., Mueller, B., Sickmann, A., and Walz, G. (2009). Tyrosine phosphorylation modulates the activity of TRPV4 in response to defined stimuli. J. Biol. Chem. *284*, 2923-2933.

33. Lutz, W., Lingle, W.L., McCormick, D., Greenwood, T.M., and Salisbury, J.L. (2001). Phosphorylation of centrin during the cell cycle and its role in centriole separation preceding centrosome duplication. J. Biol. Chem. *276*, 20774-80.

34. Lukasiewicz, K.B., Greenwood, T.M., Negron, V.C., Bruzek, A.K., Salisbury, J.L., and Lingle, W.L. (2011). Control of centrin stability by Aurora A. PLoS One *6*, e21291.

35. Lin, A., Makushok, T., Diaz, U., and Marshall, W. F. (2018). Methods for the Study of Regeneration in Stentor. J Vis Exp. 10.3791/57759.

36. Hong, C. B., Prusti, R. K. and Song, P. S. (1987). Light-Adaptation in the Photophobic Response by Stentor-Coeruleus. Arch. Microbiol. *147*, 117-120.

37. Karlis, D., and Xekalaki, E. (2005). Mixed Poisson distributions. Int. Stat. Rev. *74*, 35-58.

38. Rider, P.R. (1961). The method of moments applied to a mixture of two exponential distributions. Ann. Math. Stat. *32*, 143-147

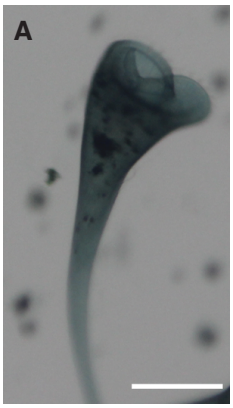
A

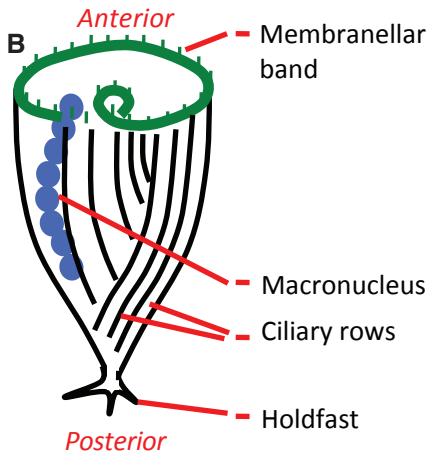
B
Anterior
Membranellar band
Macronucleus
Ciliary rows
Holdfast
Posterior

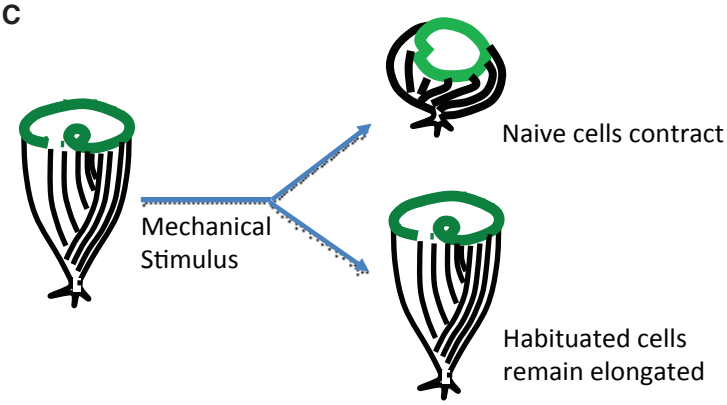
C
Naive cells contract
Mechanical Stimulus
Habituated cells remain elongated

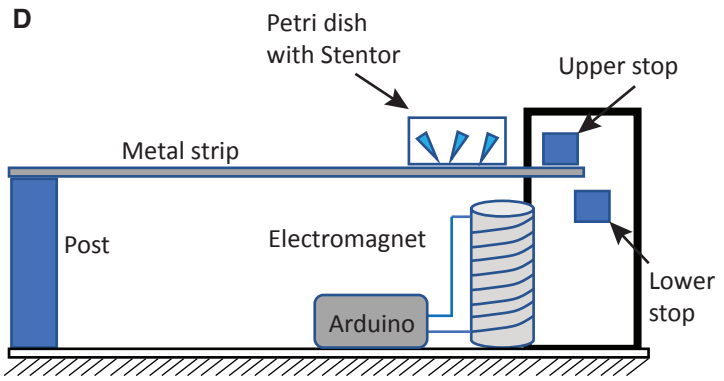
D
Petri dish with Stentor
Upper stop
Metal strip
Post
Electromagnet
Arduino
Lower stop

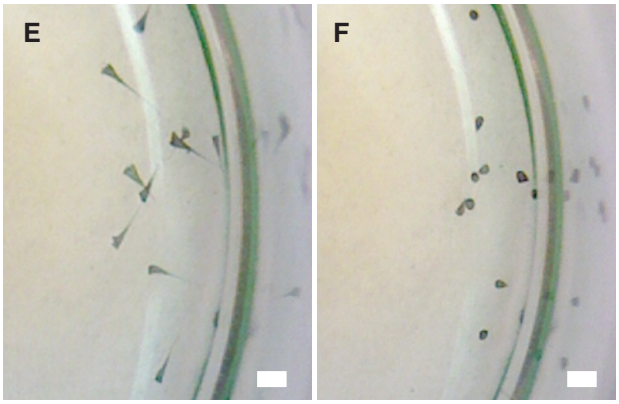
E
F

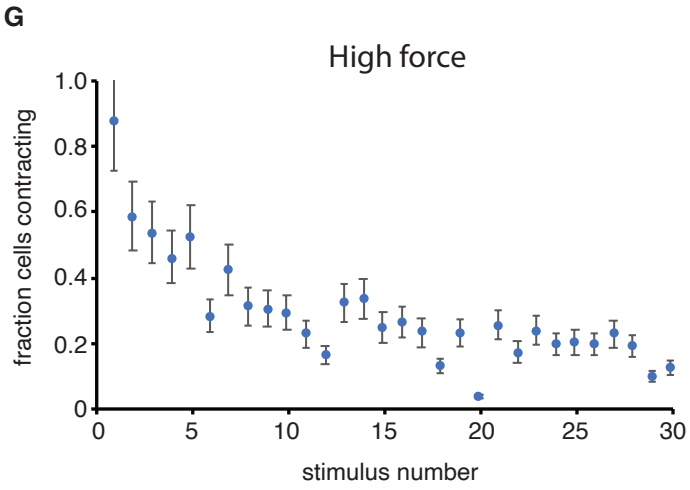
G
High force
fraction cells contracting
1.0
0.8
0.6
0.4
0.2
0
0
5
10
15
20
25
30
stimulus number

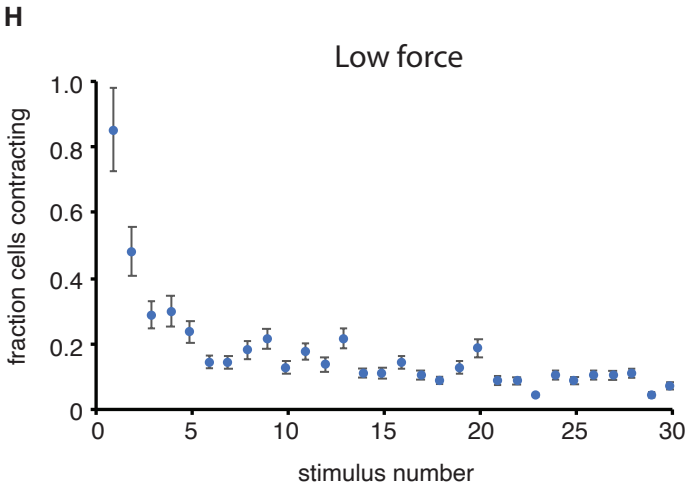
H
Low force
fraction cells contracting
1.0
0.8
0.6
0.4
0.2
0
0
5
10
15
20
25
30
stimulus number

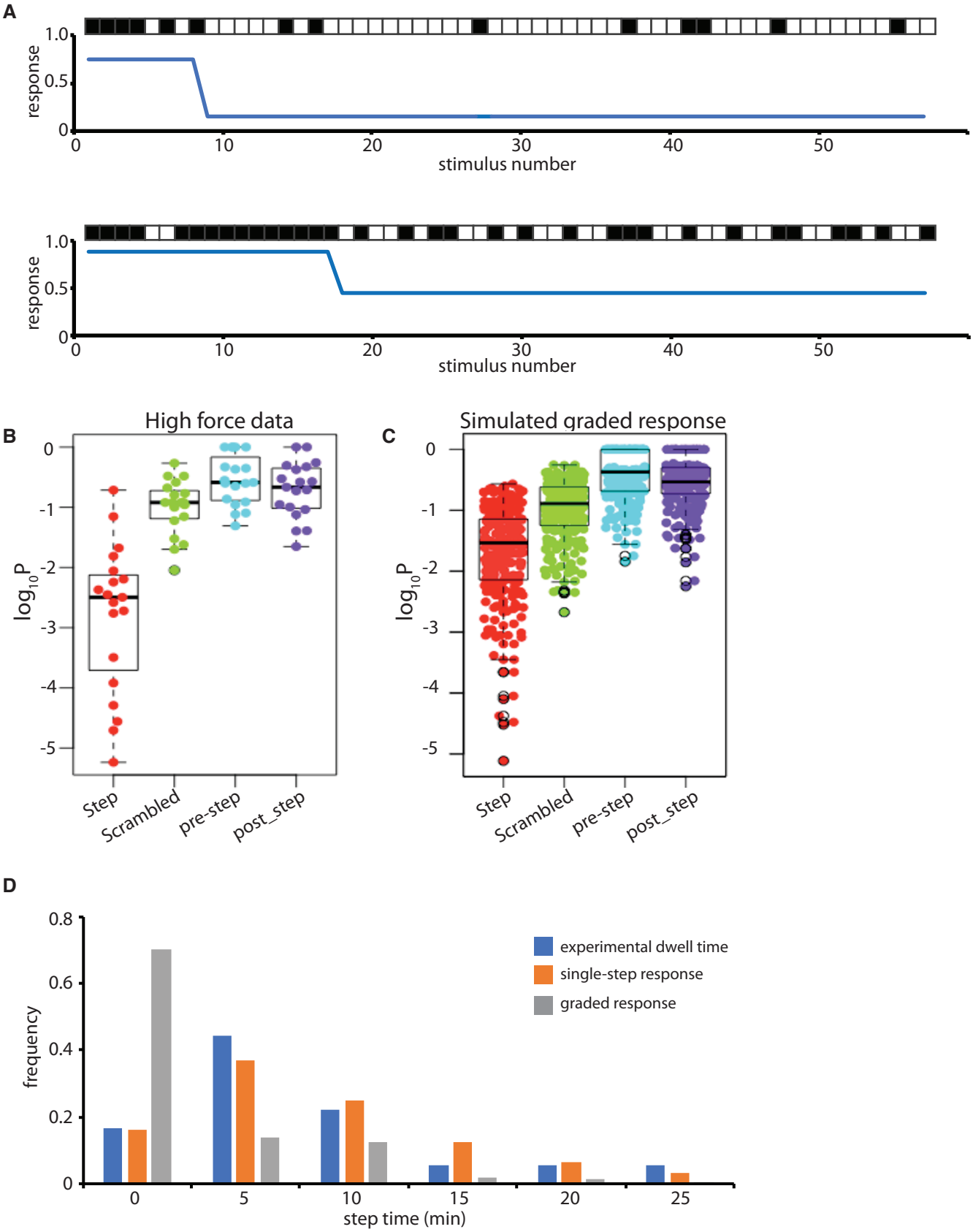
A
response
1.0
0.5
0
0
10
20
30
40
50
stimulus number
response
1.0
0.5
0
0
10
20
30
40
50
stimulus number
B
High force data
log10P
0
-1
-2
-3
-4
-5
Step
Scrambled
pre-step
post_step
C
Simulated graded response
log10P
0
-1
-2
-3
-4
-5
Step
Scrambled
pre-step
post_step
D
frequency
0.8
0.6
0.4
0.2
0
0
5
10
15
20
25
step time (min)
experimental dwell time
single-step response
graded response

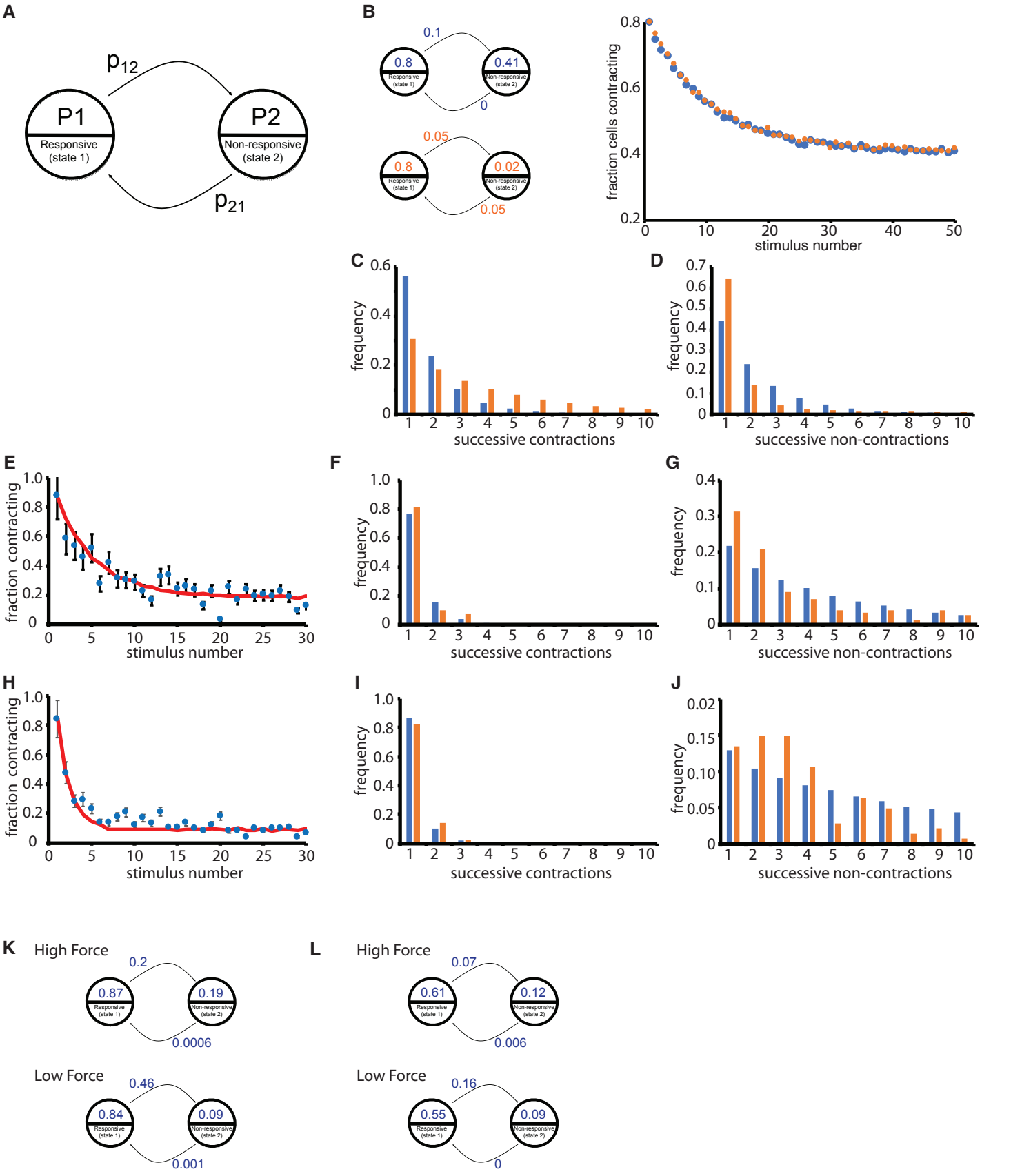
A
P1
Responsive
(state 1)
P2
Non-responsive
(state 2)
p12
p21
B
0.1
0.8
Responsive
(state 1)
0.41
Non-responsive
(state 2)
0
0.05
0.8
Responsive
(state 1)
0.02
Non-responsive
(state 2)
0.05
fraction cells contracting
stimulus number
C
frequency
successive contractions
D
frequency
successive non-contractions
E
fraction contracting
stimulus number
F
frequency
successive contractions
G
frequency
successive non-contractions
H
fraction contracting
stimulus number
I
frequency
successive contractions
J
frequency
successive non-contractions
K
High Force
0.2
0.87
Responsive
(state 1)
0.19
Non-responsive
(state 2)
0.0006
Low Force
0.46
0.84
Responsive
(state 1)
0.09
Non-responsive
(state 2)
0.001
L
High Force
0.07
0.61
Responsive
(state 1)
0.12
Non-responsive
(state 2)
0.006
Low Force
0.16
0.55
Responsive
(state 1)
0.09
Non-responsive
(state 2)
0

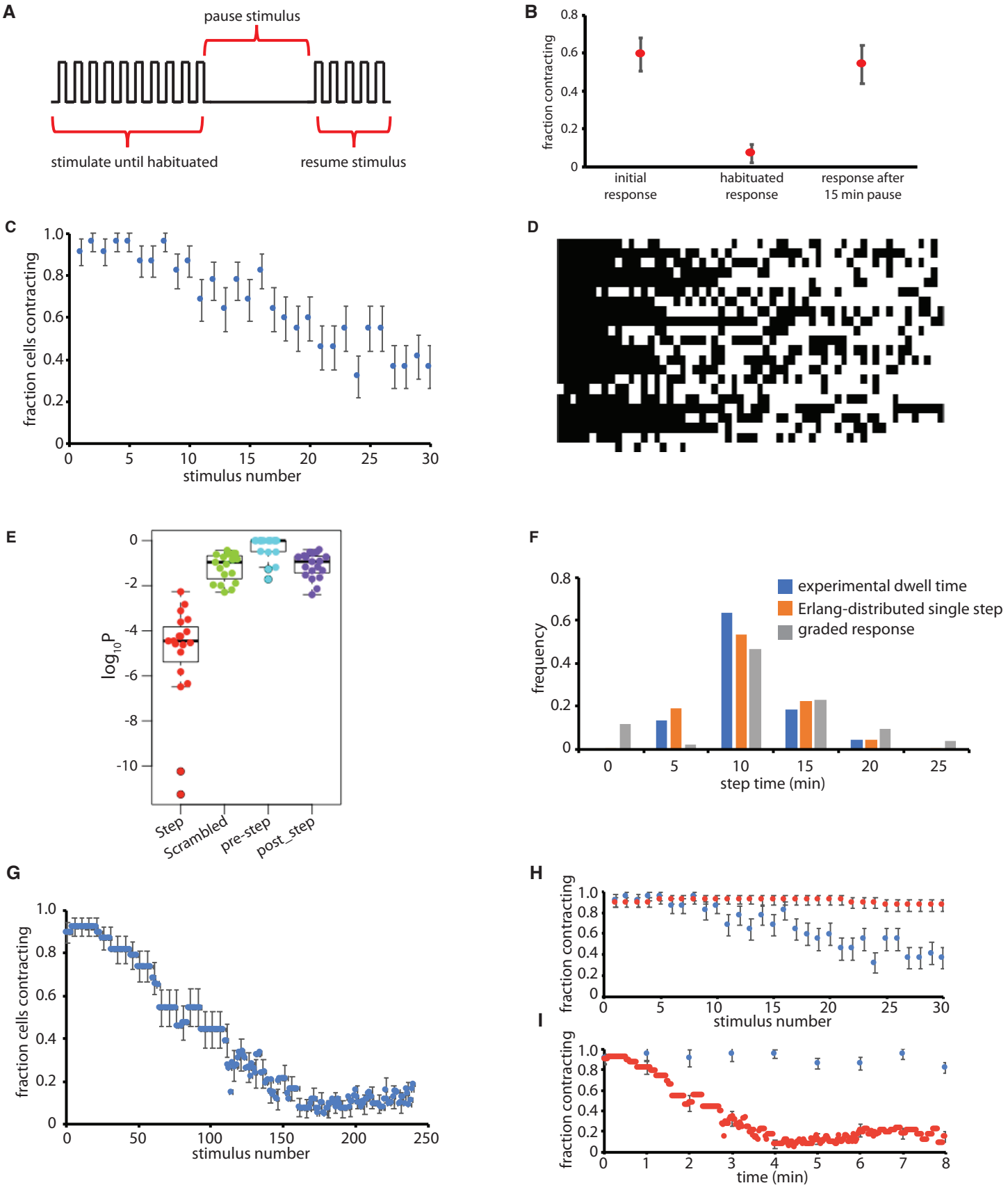
A
pause stimulus
stimulate until habituated
resume stimulus
B
fraction contracting
initial response
habituated response
response after 15 min pause
C
fraction cells contracting
stimulus number
D
E
log10 P
Step
Scrambled
pre-step
post_step
F
frequency
experimental dwell time
Erlang-distributed single step
graded response
step time (min)
G
fraction cells contracting
stimulus number
H
fraction contracting
stimulus number
I
fraction contracting
time (min)